



A Journal of



## Accepted Article

**Title:** Corner- and Side-Opened Cage Silsesquioxanes: Structural Effects on the Materials Properties

**Authors:** Hiroaki Imoto, Yukiho Ueda, Yuri Sato, Masashi Nakamura, Koji Mitamura, Seiji Watase, and Kensuke Naka

This manuscript has been accepted after peer review and appears as an Accepted Article online prior to editing, proofing, and formal publication of the final Version of Record (VoR). This work is currently citable by using the Digital Object Identifier (DOI) given below. The VoR will be published online in Early View as soon as possible and may be different to this Accepted Article as a result of editing. Readers should obtain the VoR from the journal website shown below when it is published to ensure accuracy of information. The authors are responsible for the content of this Accepted Article.

**To be cited as:** *Eur. J. Inorg. Chem.* 10.1002/ejic.201901182

**Link to VoR:** <http://dx.doi.org/10.1002/ejic.201901182>

WILEY-VCH

# Corner- and Side-Opened Cage Silsesquioxanes: Structural Effects on the Materials Properties

Hiroaki Imoto,<sup>[a,b]</sup> Yukiho Ueda,<sup>[a]</sup> Yuri Sato,<sup>[a]</sup> Masashi Nakamura,<sup>[c]</sup> Koji Mitamura,<sup>[c]</sup> Seiji Watase,<sup>[c]</sup> and Kensuke Naka\*<sup>[a,b]</sup>

**Abstract:** Open-cage silsesquioxane, in which traditional closed-cage silsesquioxane is partially hydrolyzed, is a promising class of building blocks for constructing organic-inorganic hybrid. It has advantages in high thermal stability, low crystallinity, transparency, designability, etc. Although the structural effects of closed-cage silsesquioxanes have been elucidated in detail so far, those of open-cages have never been studied. Herein, we synthesized corner- and side-opened cage silsesquioxanes having carbazole units at the open moieties. The former was amorphous in the solid state and polymer matrix, while the latter formed crystalline structures. These different packing structures caused significant difference in the performance as an emission layer of organic light emitting device.

## Introduction

Silsesquioxanes ((RSiO<sub>1.5</sub>)<sub>n</sub>) are promising building blocks for constructing organic-inorganic hybrid materials because the organic substituents (R) are incorporated to the siloxane networks.<sup>[1]</sup> In general, the structures of silsesquioxanes are classified into three types, *i.e.*, random, ladder,<sup>[2]</sup> and cage<sup>[3]</sup> structures. Cage silsesquioxanes, denoted as polyhedral oligomeric silsesquioxanes (POSS), are particularly suitable for precisely designed materials; structural control of random silsesquioxanes is difficult, and synthesis of ladder silsesquioxanes requires troublesome procedures. POSSs are further classified into two types such as closed and open types, called here CC-POSS (completely condensed POSS, Chart 1a) and IC-POSS (incompletely condensed POSS, Chart 1b),<sup>[4]</sup> respectively. CC-POSS has been traditionally utilized for reinforcement of organic materials; main-chain,<sup>[5,6]</sup> side-chain,<sup>[7]</sup> cross-linking agents,<sup>[8]</sup> and nano-fillers.<sup>[9]</sup> In general, incorporation of CC-POSS into polymers can improve mechanical properties and thermal stability.

Materials based on IC-POSS are recently emerging research subjects of interest. Corner- and side-opened IC-POSSs are commercially available. Conventionally, corner-opened IC-POSS has been recognized as a precursor for mono-functionalized CC-POSS.<sup>[4a,7,10]</sup> On the other hand, the silanol groups of IC-POSS are excellent tools to three-dimensionally link functional units. We and other researchers reported IC-POSS materials used to the main-chain polymers,<sup>[11]</sup> cross-linking agents,<sup>[12]</sup> nano-fillers,<sup>[13]</sup> amphiphilic molecules,<sup>[14]</sup> etc. It is notable that dispersibility of IC-POSS is higher than the corresponding CC-POSS, while they have similar thermal stabilities.<sup>[14a]</sup>

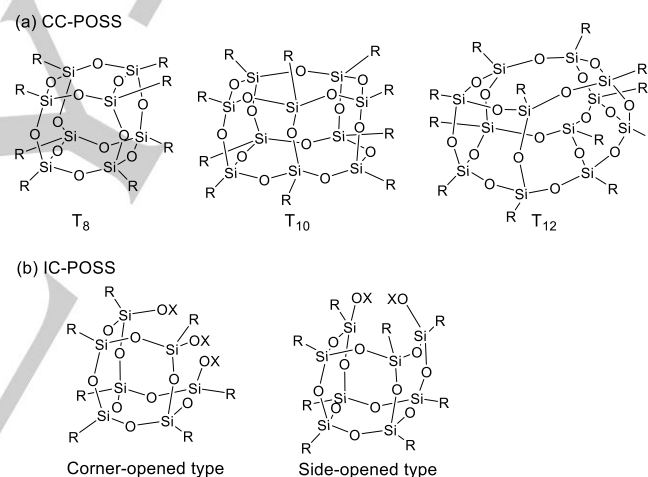


**Chart 1.** Chemical structures of (a) CC- and (b) IC-POSSs.

Here we compare the dispersibility and thermal stability of CC-POSS and IC-POSS. Among CC-POSS structures, octa-, deca-, and dodecameric silsesquioxanes (T<sub>8</sub>, T<sub>10</sub>, and T<sub>12</sub>, respectively) were also compared in various perspectives: crystallinity, porosity, photophysical properties, etc.<sup>[15]</sup> It is evident that a cage structures of IC-POSS are crucial to the resulting materials properties.<sup>[16]</sup> Nevertheless, the structural effects of the open-cage core have never been studied between IC-POSS derivatives such as corner- and side-opened IC-POSSs. For this end, it is rational that introduction of emissive units into the open moieties is an effective strategy because the effects of the structural difference can be evaluated through the observation of the photophysical properties. In this work, we thus synthesized carbazole-substituted corner- and side-opened IC-POSSs (**2a** and **2b**, respectively), and elucidated relationships between their structures and materials properties.

[a] Dr. H. Imoto, Y. Ueda, Y. Sato, Prof. Dr. K. Naka  
Faculty of Molecular Chemistry and Engineering, Graduate School  
of Science and Technology  
Kyoto Institute of Technology  
Goshokaido-cho, Matsugasaki, Sakyo-ku, Kyoto 606-8585, Japan  
E-mail: kenaka@kit.ac.jp  
Homepage: [http://www.cis.kit.ac.jp/~kenaka/index\\_eng.html](http://www.cis.kit.ac.jp/~kenaka/index_eng.html)

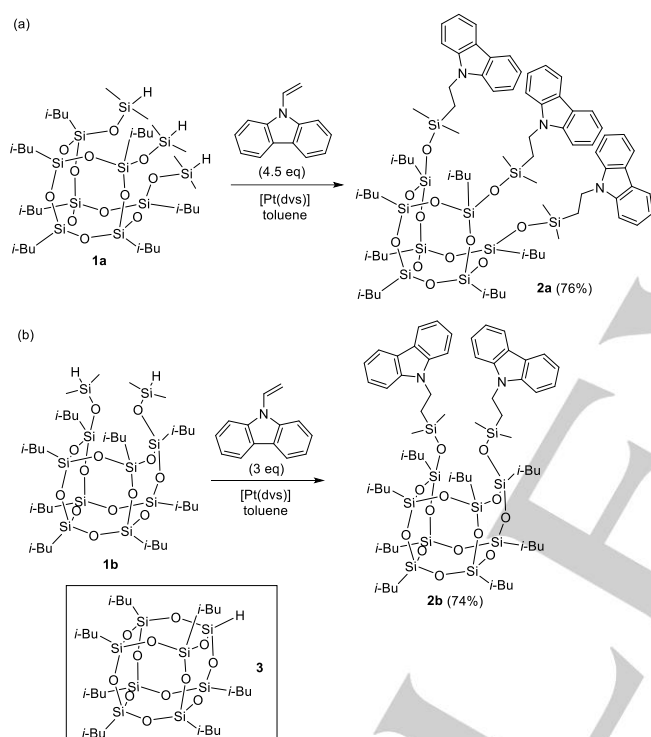
[b] Materials Innovation Lab, Kyoto Institute of Technology,  
Goshokaido-cho, Matsugasaki, Sakyo-ku, Kyoto 606-8585, Japan.

[c] Dr. M. Nakamura, Dr. K. Mitamura, Dr. S. Watase  
Osaka Research Institute of Industrial Science and Technology,  
Morinomiya Center  
1-6-50 Morinomiya, Joto-ku, Osaka 536-8553, Japan

Supporting information for this article is given via a link at the end of the document.

## Results and Discussion

The syntheses of **2a** and **2b** are shown in Scheme 1. Corner- and side-opened IC-POSSs having dimethylsilyl capping groups (**1a**<sup>[14a]</sup> and **1b**<sup>[17]</sup> respectively) were prepared from commercially available trisilanol- and disilanol-IC-POSSs in using to our published procedure.<sup>[14a]</sup> Hydrosilylation of **1** with 9-vinylcarbazole was carried out in the presence of Karstedt's catalyst ([Pt(dvs)], dvs = 1,3-divinyl-1,1,3,3-tetramethyldisiloxane). The products were purified using a preparative HPLC using chloroform (CHCl<sub>3</sub>) as the eluent. The residual metal species were removed using an amine-modified metal scavenger. The chemical structures of **2** were determined by NMR spectroscopy and MALDI-TOFMS, and the purities were confirmed by size exclusion chromatography (SEC).



**Scheme 1.** Syntheses of carbazole-substituted (a) corner- and (b) side-opened IC-POSSs, and chemical structure of **3**.

The thermal properties of IC-POSSs **1** and heptaisobutyl-CC-POSS **3** were examined by thermogravimetric analysis (TGA) and differential scanning calorimetry (DSC).<sup>[18]</sup> The temperatures at which the samples lost 5 and 10 wt% from the original mass ( $T_{d5}$  and  $T_{d10}$ , respectively), and melting points ( $T_m$ s) are summarized in Table 1 and Figure S11. The  $T_{d5}$ s and  $T_{d10}$ s of **1** were comparable to those of **3**, meaning that thermal stability was not affected by opening the POSS core. On the other hand, the  $T_m$ s of **1** were significantly lower than that of **3** due to the open-cage structures; in particular, **1a** is liquid at room temperature.<sup>[14a]</sup> This is because the crystallinity of POSS was lowered by the reduced symmetry of core structures (*vide infra*).

**Table 1.** Thermal properties of **1** and **3**.

	TGA		DSC
	$T_{d5}$ [°C] <sup>[a]</sup>	$T_{d10}$ [°C] <sup>[a]</sup>	$T_m$ [°C] <sup>[b]</sup>
<b>1a</b>	200	213	-18 <sup>[c]</sup>
<b>1b</b>	226	239	66
<b>3</b>	208	218	135

[a] The temperatures at which the samples lost 5 and 10 wt% from the original mass ( $T_{d5}$  and  $T_{d10}$ , respectively). [b] Melting point. [c] Cited from reference 14a.

The optical properties of **2** were investigated as shown in Figure 1 and Table S1. The UV-vis absorption (Figure 1a) and photoluminescence (PL) spectra (Figure 1b) of **2** and 9-ethylcarbazole were measured in THF solutions ([carbazole unit] =  $5.0 \times 10^{-5}$  M). The spectra of **2** and 9-ethylcarbazole were quite similar, meaning that the carbazole units on the IC-POSSs have negligible interactions in the ground and excited states. We further examined donor-acceptor interactions between the carbazole moieties and *m*-dinitrobenzene, but no significant differences were observed (for detail, see Figure S12). In the case of the solid state (Figure 1c), the PL spectra of **2** were also quite similar, though that of 9-ethylcarbazole showed red-shifted spectra by 39 nm (**2a**) and 40 nm (**2b**); the carbazole units of **2** and 9-ethylcarbazole were partially and totally eclipsed, respectively.<sup>[19]</sup> These results indicate that there are no structural effects of the open-cages on the photophysical properties in solution and solid states.

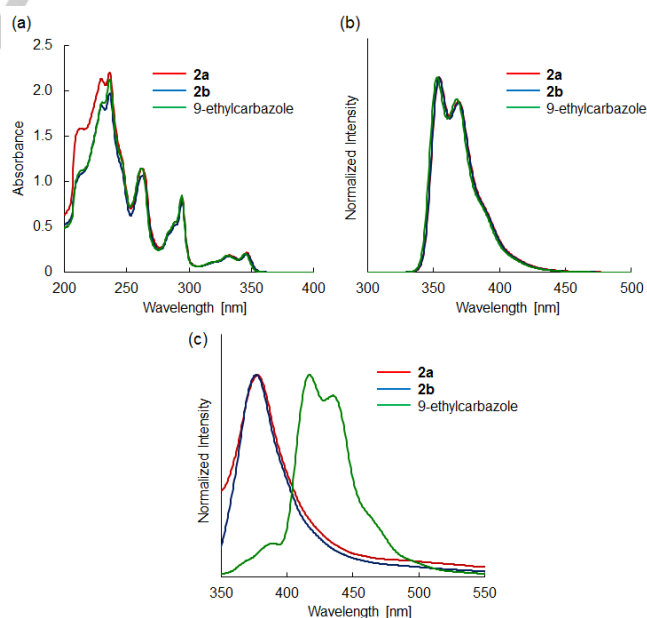


**Figure 1.** (a) UV-vis and (b) PL spectra of **2** and 9-ethylcarbazole in THF solutions ([carbazole unit] =  $5.0 \times 10^{-5}$  M). (c) PL spectra of **2** and 9-ethylcarbazole in the solid states.

During the investigation on the solid state emission properties, we found that the appearances of **2** in their solid states were different. That is, films of **2a** were transparent (Figure 2a), whereas **2b** formed a turbid film (Figure 2b). We thus conducted scanning electron microscope (SEM) studies for the films of **2** (Figure 2c and 2d). The film of **2a** is homogeneous, while aggregates of sub-micrometer to micrometer order were observed for **2b**. Powder X-ray diffraction (XRD) patterns indicate that **2b** has much higher crystallinity than **2a**. This corresponds to DSC measurements shown in Table 1; side-opened IC-POSS **1b** is crystalline at room temperature while corner-opened IC-POSS **1a** is a liquid.

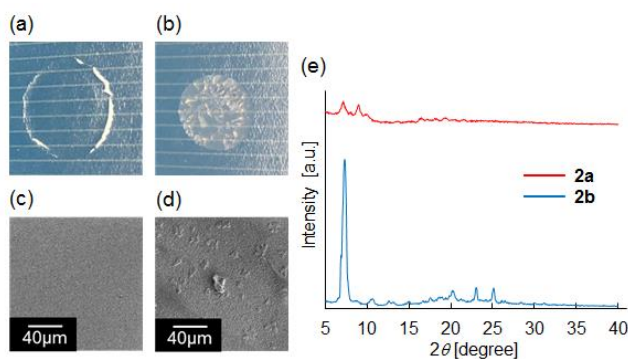


**Figure 2.** (a, b) Photographs and (c, d) SEM images the films of **2**, which were fabricated by drop-casting from  $\text{CHCl}_3$  solutions (75 g/L). (e) Powder XRD patterns of **2**.

This result motivated us to investigate the electronic properties that might depend on the morphologies of hole-transporting carbazole groups in each IC-POSS.<sup>[20]</sup> Since the performance of light-emitting devices (OLEDs) depend on the luminescent and electronic properties of the light emitting layer, we fabricated devices using IC-POSSs **2** and evaluated their performance. In order to apply **2** as emission centers to OLEDs, they were made into thin films by hybridizing with poly(phenylsilsesquioxane) (PPSQ). The ratio of [carbazole group] to [phenyl group] was 2 to 3 for both the hybrid films. Device configurations were Al/TAZ/**2**-PPSQ/PEDOT/ITO. Both devices were successfully fabricated and showed electroluminescence. In these devices, the carbazole group can play a role as a recombination site for holes and electrons as well as an emission center. Comparing to two devices, the maximum current density and the maximum luminance of the device containing **2a** was approximately twice those of a device containing **2b** (Figures 3 and S13). This result strongly suggests that the difference in crystallinity greatly affects device performance. In particular, low crystallinity of corner-opened IC-POSS core leads to good device performance, which may be

due to the mobility and flexibility of carbazole groups in the hybrid.

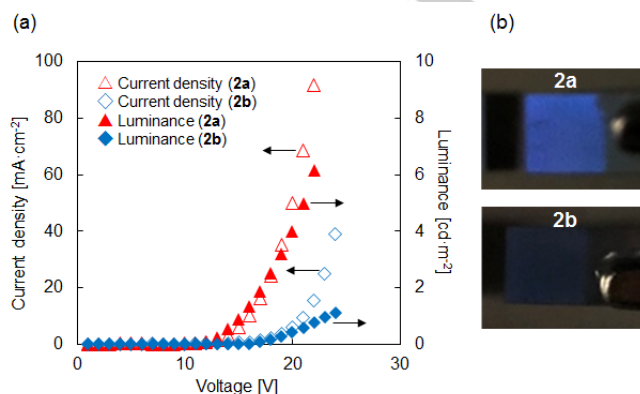


**Figure 3.** (a) Current density and luminance curves versus driving voltage and (b) photographs of OLEDs using PPSQ-composites with **2a** and **2b** as emission centers.

XRD measurements of the PPSQ composite films were conducted to understand the difference in morphology in the devices between **2a** and **2b** (Figure S10). The XRD of the **2a**-PPSQ film shows it was amorphous, whereas that of **2b**-PPSQ film revealed crystals of **2b**. The grain boundaries of **2b** might inhibit charge transfer in the composite film. Raman spectroscopy is a useful technique for comparing crystallinity, and gives a sharp peak with a narrow half width at high crystallinity. Therefore, to compare the difference in crystallinity of the IC-POSS cores, Raman measurements were performed in solution and in the solid state. A peak attributed to the stretching mode of the biphenyl skeleton derived from the carbazole group of interest and was observed near  $1630 \text{ cm}^{-1}$ . Figure S14a shows those peaks derived from **2a** and **2b** in THF solutions. The full width at half maxima (FWHM) of the peaks of **2a** and **2b** are similar. Thus the carbazole groups of **2a** and **2b** have similar environments in solution. On the other hand, the FWHM of the peak due to **2a** in the solid state was larger than that of **2b** (Figure S14b). The periodicity of the carbazole group of **2a** in the solid state is more disordered than that of **2b**, because of the lower crystallinity due to a corner-opened IC-POSS core. This observation is consistent with the X-ray diffraction measurements.

Finally, the symmetrical difference between corner- and side-opened IC-POSSs and CC-POSS was evaluated based on the structures which were optimized by density functional theory (DFT) calculations (Figure 4).<sup>[21]</sup> The structures were simplified for the calculation cost; the isobutyl and carbazoleethyl groups were replaced by methyl groups; the virtual molecules were defined as **2a'** (corner-opened IC-POSS), **2b'** (side-opened IC-POSS), and **3'** (CC-POSS). The calculations were performed at the B3LYP/6-31G(d) level of theory with the Gaussian 09.<sup>[22]</sup> The centroids of the silicon atoms that form the cage structures were calculated by the Cartesian coordinates. The symmetry of the cages was evaluated by the variance ( $\sigma$ ) of the distance

between the centroid and each silicon atom. In the case of **3'**,  $\sigma$  was approximately 0 due to the highly symmetrical cubic structure. On the other hand, the corner- and side-opened cages possessed relatively large  $\sigma$  values, and the  $\sigma$  value of **2a'** ( $\sigma = 0.446$ ) was significantly larger than that of **2b'** ( $\sigma = 0.344$ ). This means that the corner-opened structure possesses lower symmetry than the side-opened structure, well corresponding to the experimental results that show the lower crystallinity of **2a**.

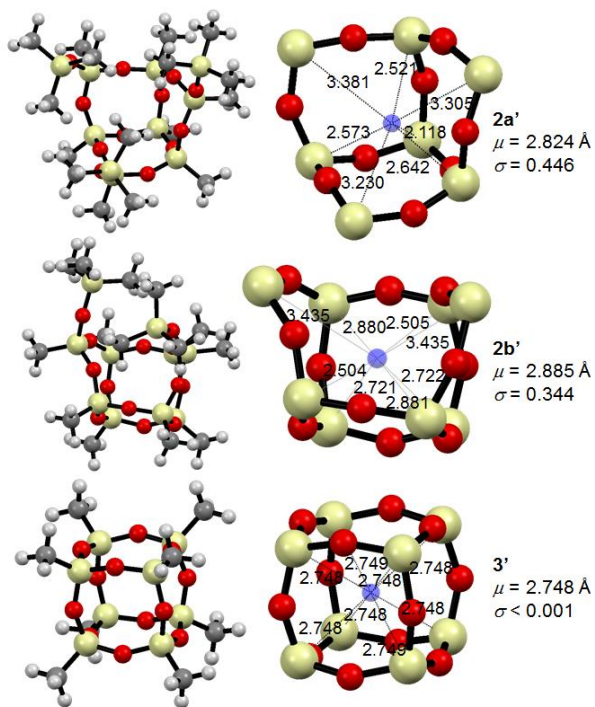


**Figure 4.** (Left) Optimized structures of **2a'**, **2b'**, and **3'** (yellow: Si, red: O, grey: C, white: H). (Right) Part of cage core structures and distances (Å) between centroid (blue dot) and silicon atoms. Average ( $\mu$ ) and variance ( $\sigma$ ) of the distances are shown.

## Conclusions

IC-POSS is an excellent tool to design organic-inorganic hybrid molecules because the silanol groups can be used for incorporation of the functional units into the stable inorganic core. In the present work, carbazole-substituted corner- and side-opened IC-POSSs **2** were synthesized to demonstrate their differences in the structures and materials properties. The structures of IC-POSS cores made negligible differences in the photophysical properties in solutions and the solid states, considering the UV-vis and PL spectra. On the other hand, the molecular packings in the solid states were significantly different; **2a** was amorphous, while **2b** formed the crystalline structure. The high dispersibility of **2a** realized more efficient emission in the OLED, whereas the crystallization of **2b** inhibited the charge transport. This is the first study on the structural effects of the IC-POSSs on photophysical properties. The molecular design

which the present study elucidated has opened new avenue to development of silsesquioxane materials.

## Experimental Section

### 1. Materials

Tetrahydrofuran (THF), chloroform ( $\text{CHCl}_3$ ), triethylamine ( $\text{NEt}_3$ ), and methanol (MeOH) were purchased from Nacalai Tesque (Kyoto, Japan). Toluene, *n*-hexane, magnesium sulfate anhydrous ( $\text{MgSO}_4$ ), and distilled water were purchased from Fujifilm Wako Pure Chemical Industry (Osaka, Japan). Chlorodimethylsilane, 9-vinylcarbazole, 9-ethylcarbazole, and *m*-dinitrobenzene were purchased from Tokyo Chemical Industry (Tokyo, Japan). Xylene solution (0.1 M) of platinum(0)-1,3-divinyl-1,1,3,3-tetramethyldisiloxane (Pt(dvs)) was purchased from Sigma-Aldrich (Hattiesburg, Mississippi, US). Heptaisobutyl trisilanol POSS and octaisobutyl disilanol POSS were purchased from Hybrid Plastics Inc (Hattiesburg, Mississippi, US). Metal scavenger, SiliaMetS(R) Triamine (Particle size: 40–63  $\mu\text{m}$ , Pore diameter: 60 Å, Particle shape: Irregular Silica Gel) was purchased from SiliCycle, Inc (Quebec City, Québec, Canada). Heptaisobutyl POSS (**3**) was prepared according to the literature procedure.<sup>[14a]</sup>

### 2. Method

$^1\text{H}$  (400MHz),  $^{13}\text{C}$  (100MHz), and  $^{29}\text{Si}$  (80MHz) nuclear magnetic resonance (NMR) spectra were recorded on a Bruker DPX-400 spectrometer (Bruker Biospin GmbH, Rheinstetten, Germany) in  $\text{CDCl}_3$  using  $\text{Me}_4\text{Si}$  as an internal standard. The following abbreviations are used: t, triplet; q, quartet; quint, quintet; sext, sextet; sep, septet; m, multiplet. Molecular weights were determined by size exclusion chromatography (SEC) of LC-6AD (Shimadzu, Kyoto, Japan) with a Shodex KF-803L (Showa Denko, Tokyo, Japan) column and a refractive index detector RID-20A (Shimadzu, Kyoto, Japan). Preparative high-performance liquid chromatography (HPLC) for purification was performed on LC-6AD (Shimadzu, Kyoto, Japan) with a KF-2001 using chloroform as an eluent. Matrix assisted laser desorption ionization time-of-flight mass spectrometry (MALDI-TOF-MS) was recorded on a Bruker Autoflex II instrument (Bruker Daltonics, Billerica, MA, USA): *trans*-2-[3-(4-*tert*-butylphenyl)-2-methyl-2-propenylidene]malononitrile (DCTB) matrix (20 mg/mL in  $\text{CHCl}_3$ ) and sodium trifluoroacetate cationizing agents (1 mg/mL in THF). TGA and DSC measurements were performed by Shimadzu DTG-60 and DSC-60 Plus (Shimadzu, Kyoto, Japan), respectively, under nitrogen atmosphere at a heating rate of 10  $^\circ\text{C}/\text{min}$ . UV-vis absorption spectra were recorded on a JASCO spectrophotometer V-670 KNN (JASCO, Tokyo, Japan). Emission and excitation spectra were obtained on an FP-8500 (JASCO), and absolute PL quantum yields ( $\Phi$ ) were determined using a JASCO ILFC-847S; the quantum yield of quinine sulfate reference was 0.52, which is in agreement with the literature value.<sup>[23]</sup> X-ray diffractometry (XRD) studies were performed on a Rigaku Smartlab X-ray diffractometer with  $\text{Cu K}\alpha$  radiation ( $\lambda = 1.5406$  Å) in the  $2\theta/\theta$  mode at room temperature. The  $2\theta$  scan data were collected at 0.01 $^\circ$  intervals and the scan speed was 10 $^\circ$  ( $2\theta$ ) / min. The surface of the films was observed using a VE-8800 scanning electron microscope (SEM) (KEYENCE, Osaka, Japan). Raman spectra were taken using a HORIBA Raman spectrometer LabRAM HR Evolution (Horiba, Kyoto, Japan). The laser excitation wavelength used in these studies was 532 nm and the output was 15 mW in the solid state or 30 mW in solution, respectively. The wavenumber resolution was 0.4 to 0.5  $\text{cm}^{-1}$ .

### 3. Synthetic procedure and characterization data

**Tris(dimethylsiloxy)heptaisobutyl IC-POSS (1a).**<sup>[14a]</sup> A THF solution (30 mL) of heptaisobutyl trisilanol POSS (2.0 g, 2.53 mmol) and Et<sub>3</sub>N (2.45 mL, 17.7 mmol) was cooled to 0 °C under N<sub>2</sub> atmosphere, and chlorodimethylsilane (1.23 mL, 11.4 mmol) was added dropwise. After stirring at 0 °C for 1 h, the reaction mixture was warmed to room temperature for 3h, and the reaction was quenched by addition of distilled water. The volatiles were removed *in vacuo*, and the residue was dissolved in *n*-hexane. The solution was washed with distilled water, and the organic layer was dried over MgSO<sub>4</sub>. The solvent was removed *in vacuo*, and the residue was subjected to reprecipitation from the CHCl<sub>3</sub> solution to methanol to obtain **1a** (2.15 g, 2.22 mmol, 87%) as white solids. <sup>1</sup>H-NMR (CDCl<sub>3</sub>, 400 MHz) δ 4.74 (sep, *J* = 2.86 Hz, 3H), 1.89–1.79 (m, 7H), 0.96 (quint, *J* = 3.56 Hz, 42H), 0.56(t, *J* = 6.47 Hz, 14H), 0.22 (q, *J* = 3.33 Hz, 18H) ppm; <sup>13</sup>C-NMR (CDCl<sub>3</sub>, 100 MHz) δ 26.0, 25.8, 25.6, 24.6, 24.1, 24.0, 23.9, 23.6, 22.4, 0.6 ppm; <sup>29</sup>Si-NMR (CDCl<sub>3</sub>, 80 MHz) δ -5.4, -67.1, -67.6, -68.0 ppm.

**Bis(dimethylsiloxy)octaisobutyl IC-POSS (1b).** A THF solution (30 mL) of octaisobutyl disilanol POSS (2.0 g, 2.24 mmol) and Et<sub>3</sub>N (2.18 mL, 15.7 mmol) was cooled to 0 °C under N<sub>2</sub> atmosphere, and chlorodimethylsilane (0.73 mL, 6.73 mmol) was added dropwise. After stirring at 0 °C for 1 h, the reaction mixture was warmed to room temperature for 3h, and the reaction was quenched by addition of distilled water. The volatiles were removed *in vacuo*, and the residue was dissolved in *n*-hexane. The solution was washed with distilled water, and the organic layer was dried over MgSO<sub>4</sub>. The solvent was removed *in vacuo*, and the residue was subjected to reprecipitation from the CHCl<sub>3</sub> solution to methanol to obtain **1b** (1.97 g, 1.95 mmol, 85%) as white solids. <sup>1</sup>H-NMR (CDCl<sub>3</sub>, 400 MHz) δ 4.73 (sep, *J* = 2.77 Hz, 2H), 1.90–1.80 (m, 8H), 1.02–0.90 (m, 48H), 0.57 (sext, *J* = 2.07 Hz, 16H), 0.28–0.18 (m, 12H) ppm; <sup>13</sup>C-NMR (CDCl<sub>3</sub>, 100 MHz) δ 25.9, 25.9, 25.8, 25.7, 24.6, 24.0, 23.9, 23.8, 23.5, 22.5, 0.59 ppm; <sup>29</sup>Si-NMR (CDCl<sub>3</sub>, 80 MHz) δ -5.17, -65.8, -66.0, -68.1 ppm. The NMR spectral data corresponds the literature.<sup>[17]</sup>

**Tris(carbazolethyl)dimethylsiloxyheptaisobutyl IC-POSS (2a).** To a toluene solution (7.0 mL) of **1a** (0.70 g, 0.72 mmol) and 9-vinylcarbazole (0.63 g, 3.26 mmol) was added a xylene solution of Pt(dvs) (0.1 M, 29 μL) under N<sub>2</sub> atmosphere. After stirring at 80 °C for 6 h, the volatiles were removed *in vacuo*. The residue was subjected to preparative HPLC, and the residual metal species were adsorbed to metal scavenger, SiliaMetS(R) Triamine. The solvents were removed *in vacuo* to obtain **2a** (0.85 g, 0.55 mmol, 76%) as white viscous solids. <sup>1</sup>H-NMR (CDCl<sub>3</sub>, 400 MHz) δ 8.11–7.17 (m, 24H), 4.40–4.28 (m, 6H), 1.98–1.87 (m, 7H), 1.18–1.10 (m, 6H), 1.07–0.96 (m, 42H), 0.66 (sext, *J* = 6.65 Hz, 14H), 0.27–0.09 (m, 18H) ppm; <sup>13</sup>C-NMR (CDCl<sub>3</sub>, 100 MHz) δ 139.8, 125.5, 123.0, 120.4, 118.7, 108.5, 38.2, 26.1, 25.9, 25.7, 25.1, 24.3, 24.1, 23.9, 23.8, 22.4, 18.3, 0.53 ppm; <sup>29</sup>Si-NMR (CDCl<sub>3</sub>, 80 MHz) δ 7.49, -67.0, -67.0, -67.1 ppm. MALDI-TOFMS (*m/z*): calculated for C<sub>76</sub>H<sub>117</sub>O<sub>12</sub>N<sub>3</sub>Si<sub>10</sub> [M]<sup>+</sup>: 1543.63, found 1543.63.

**Bis(carbazolethyl)dimethylsiloxyoctaisobutyl IC-POSS (2b).** To a toluene solution (2.0 mL) of **1b** (0.20 g, 0.20 mmol) and 9-vinylcarbazole (0.12 g, 0.60 mmol) was added a xylene solution of Pt(dvs) (0.1 M, 14 μL) under N<sub>2</sub> atmosphere. After stirring at 80 °C for 6 h, the volatiles were removed *in vacuo*. The residue was subjected to preparative HPLC, and the residual metal species were adsorbed to metal scavenger, SiliaMetS(R) Triamine. The solvents were removed *in vacuo* to obtain **2a** (0.20 g, 0.15 mmol, 74%) as white solids. <sup>1</sup>H-NMR (CDCl<sub>3</sub>, 400 MHz) δ 8.03–7.09 (m, 16H), 4.36–4.25 (m, 4H), 1.89–1.72 (m, 8H), 1.11–0.99 (m, 4H), 0.95–0.81 (m, 48H), 0.60–0.44 (m, 16H), 0.22–0.04 (m, 12H) ppm; <sup>13</sup>C-NMR (CDCl<sub>3</sub>, 100 MHz) δ 139.8, 125.5, 123.0, 120.4, 118.6, 108.5, 38.2, 26.1, 25.9, 25.8, 25.8, 25.1, 24.2, 24.0, 23.8, 23.6, 22.5, 18.4, 0.52 ppm; <sup>29</sup>Si-NMR (CDCl<sub>3</sub>, 80 MHz) δ 7.62, -65.3, -65.7, -67.4 ppm. MALDI-

TOFMS (*m/z*): calculated for C<sub>64</sub>H<sub>108</sub>O<sub>13</sub>N<sub>2</sub>Si<sub>10</sub> [M]<sup>+</sup>: 1392.55, found 1392.56.

#### 4. Evaluation of OLED devices

**Preparation of PPSQ.** To a THF solution of phenyltrimethoxysilane (0.22 g, 0.10 mmol), small amount of formic acid as a catalyst and four equivalents of water (0.007 g, 0.40 mmol) were added. The condensation of the reaction mixture was carried out in a glass vessel upon stirring at 90 °C for 1 h, and then at 120 °C for another 1 h, giving a solid product. CHCl<sub>3</sub> solutions (0.5 wt%) of **2a**, **2b**, and PPSQ were separately prepared, and they were mixed ([carbazole group]: [phenyl group] = 2: 3) for fabrication of the OLEDs.

**Device fabrication.** The OLED was fabricated on the ITO glass by the following procedure. Firstly, the hole transporting PEDOT: PSS and hybrid emitting layers were deposited sequentially by spin-coating. These coatings were post-baked using hot-plate heated at 100 degree. Next, electron transporting TAZ layer and Al electrode were deposited sequentially under high vacuum environment (< 3.0 × 10<sup>-3</sup> Pa) by thermal evaporation onto spin-coated substrates with a speed of 0.1–0.3 nm/s. The thickness of the vacuum deposition layers were controlled by the quartz crystal unit. The emission area of the device was 0.16 cm<sup>2</sup> as determined by the overlap area of the anode and the cathode. Device current density-voltage-luminance characteristics were measured without protective encapsulation at ambient conditions using a computer-controlled ADCMT 6241A DC voltage current source / monitor attached with a Konica Minolta Chroma meter CS-100A. The EL spectra were recorded by Hitachi F4500 fluorescence spectrophotometer.

#### Acknowledgments

This work was supported by JSPS KAKENHI Grant Number JP18K19114. H. I. acknowledges Grant-in-Aid for Young Scientists (B) (JSPS KAKENHI Grant Number JP17K14530). We thank Prof. Tsuyoshi Kawai and Ms. Yoshiko Nishikawa of Nara Institute of Science and Technology for measuring MALDI-TOF-MS supported by Nanotechnology Platform.

**Keywords:** Luminescence • Silicon • Cage compounds • Density functional calculations • X-ray diffraction

- [1] R. H. Baney, M. Itoh, A. Sakakibara, T. Suzuki, *Chem. Rev.* **1995**, *95*, 1409.
- [2] (a) H. Matsumoto, S. Kyushin, M. Unno, R. Tanaka, *J. Organomet. Chem.* **2000**, *611*, 52; (b) M. Unno, A. Suto, H. Matsumoto, *J. Am. Chem. Soc.* **2002**, *124*, 1574.
- [3] (a) R. M. Laine, C. Zhang, A. Sellinger, L. Viculis, *Appl. Organometal. Chem.* **1998**, *12*, 715; (b) R. M. Laine, *J. Mater. Chem.* **2005**, *15*, 3725; (c) D. B. Cordes, P. D. Lickiss, F. Rataboul, *Chem. Rev.* **2010**, *110*, 2081; (d) K. Tanaka, Y. Chujo, *Bull. Chem. Soc. Jpn.* **2013**, *86*, 1231; (e) Q. Ye, H. Zhou, J. Xu, *Chem. Asian J.* **2016**, *11*, 1322; (f) K. Naka, Y. Irie, *Polym. Int.* **2017**, *66*, 187; (g) Z. Li, J. Kong, F. Wang, C. He, *J. Mater. Chem. C* **2017**, *5*, 5283; (h) H. Zhou, Q. Ye, J. Xu, *Mater. Chem. Front.* **2017**, *1*, 212; (i) H. Imoto, *Polym. J.*, **2018**, *50*, 837.
- [4] (a) J. F. Brown, L. H. Vogt, *J. Am. Chem. Soc.* **1965**, *87*, 4313; (b) F. J. Feher, S. H. Phillips, J. W. Ziller, *Chem. Commun.* **1997**, 829; (c) F. J. Feher, *Chem. Commun.* **1998**, 399; (d) F. J. Feher, R. Terroba, J. W. Ziller, *Chem. Commun.* **1999**, 2309.

- [5] (a) M. Seino, T. Hayakawa, Y. Ishida, M. Kakimoto, *Macromolecules* **2006**, *39*, 3473; (b) S. Wu, T. Hayakawa, R. Kikuchi, S. J. Grunzinger, M. Kakimoto, *Macromolecules* **2007**, *40*, 5698; (c) Md. A. Hoque, Y. Kakihana, S. Shinke, Y. Kawakami, *Macromolecules* **2009**, *42*, 3309; (d) W. Zhang, J. Xu, X. Li, G. Song, J. Mu, *J. Polym. Sci., Part A: Polym. Chem.* **2014**, *52*, 780; (e) K. Wei, L. Wang, L. Li, S. Zheng, *Polym. Chem.* **2015**, *6*, 256; (f) P. Žak, B. Dudzic, M. Dutkiewicz, M. Ludwiczak, B. Marciniak, M. Nowicki, *J. Polym. Sci., Part A: Polym. Chem.* **2016**, *54*, 1044; (g) J. Hao, Y. Wei, J. Mu, *RSC Adv.* **2016**, *6*, 87433; (h) Y.-T. Liao, Y.-C. Lin, S.-W. Kuo, *Macromolecules* **2017**, *50*, 5739.
- [6] (a) T. Maegawa, Y. Irie, H. Fueno, K. Tanaka, K. Naka, *Chem. Lett.* **2014**, *43*, 1532; (b) T. Maegawa, Y. Irie, H. Imoto, H. Fueno, K. Tanaka, K. Naka, *Polym. Chem.* **2015**, *6*, 7500; (c) T. Maegawa, O. Miyashita, Y. Irie, H. Imoto, K. Naka, *RSC Adv.* **2016**, *6*, 31751; (d) S. Fujii, S. Minami, K. Urayama, Y. Suenaga, H. Naito, O. Miyashita, H. Imoto, K. Naka, *ACS Macro Lett.* **2018**, *7*, 641.
- [7] (a) R. Goseki, A. Hirao, M. Kakimoto, T. Hayakawa, *ACS Macro Lett.* **2013**, *2*, 625; (b) L. Hong, Z. Zhang, W. Zhang, *Ind. Eng. Chem. Res.* **2014**, *53*, 10673; (c) T. Suzuki, A. Yoshida, S. Ando, K. Nagai, *Polym. Int.* **2015**, *64*, 1209; (d) F. Kato, A. Chandra, S. Horiuchi, T. Hayakawa, *RSC Adv.* **2016**, *6*, 62172; (e) T. Seshimo, Y. Utsumi, T. Dazai, T. Maehashi, T. Matsumiya, Y. Suzuki, C. Hirano, R. Maeda, K. Ohmori, T. Hayakawa, *Polym. J.* **2016**, *48*, 407.
- [8] For recent papers, see: (a) Y. Fang, H. Ha, K. Shanmuganathan, C. J. Ellison, *ACS Appl. Mater. Interfaces* **2016**, *8*, 11050; (b) X. Zhou, X. Fan, C. He, *Macromolecules* **2016**, *49*, 4236; (c) E. Carbonell, L. A. Bivona, L. Fusaro, C. Aprile, *Inorg. Chem.* **2017**, *56*, 6393; (d) D. Wang, R. Sun, S. Feng, W. Li, H. Liu, *Polymer* **2017**, *130*, 218; (e) A. Raghuvanshi, C. Strohmman, J.-B. Tissot, S. Clément, A. Mehdi, S. Richeter, L. Viau, M. Knorr, *Chem. Eur. J.* **2017**, *23*, 16479; (f) C. Xing, L. Wang, L. Xian, Y. Wang, L. Zhang, K. Xi, Q. Zhang, X. Jia, *Macromol. Chem. Phys.* **2018**, *219*, 1800042.
- [9] (a) K. Tanaka, S. Adachi, Y. Chujo, *J. Polym. Sci., Part A: Polym. Chem.* **2009**, *47*, 5690; (b) K. Tanaka, S. Adachi and Y. Chujo, *J. Polym. Sci., Part A: Polym. Chem.* **2010**, *48*, 5712; (c) J.-H. Jeon, K. Tanaka, Y. Chujo, *RSC Adv.* **2013**, *3*, 2422; (d) J.-H. Jeon, K. Tanaka, Y. Chujo, *J. Polym. Sci., Part A: Polym. Chem.* **2013**, *51*, 3583; (e) J.-H. Jeon, K. Tanaka, Y. Chujo, *J. Mater. Chem. A* **2014**, *2*, 624; (f) K. Ueda, K. Tanaka, Y. Chujo, *Polym. J.* **2016**, *48*, 1133; (g) K. Ueda, K. Tanaka, Y. Chujo, *Bull. Chem. Soc. Jpn.* **2017**, *90*, 205; (h) K. Tanaka, H. Kozuka, K. Ueda, J.-H. Jeon, Y. Chujo, *Mater. Lett.* **2017**, *203*, 62.
- [10] (a) F. J. Feher, *J. Am. Chem. Soc.* **1986**, *108*, 3850; (b) Z. Fei, K. Ibrom, F. T. Edelman, *Z. Anorg. Allg. Chem.* **2002**, *628*, 2109.
- [11] (a) M. E. Wright, D. A. Schorzman, F. J. Feher, R.-Z. Jin, *Chem. Mater.* **2003**, *15*, 264; (b) K. N. Raftopoulos, M. Jancia, D. Aravopoulou, E. Hebda, K. Pielichowski, P. Pissis, *Macromolecules* **2013**, *46*, 7378; (c) P. Wang, Y. Tang, Z. Yu, J. Gu, J. Kong, *ACS Appl. Mater. Interfaces* **2015**, *7*, 20144; (d) H. Imoto, R. Katoh, K. Naka, *Polym. Chem.* **2018**, *9*, 4108; (e) R. Katoh, H. Imoto, K. Naka, *Polym. Chem.* **2019**, *10*, 2223.
- [12] (a) M. Miyasaka, Y. Fujiwara, H. Kudo, T. Nishikubo, *Polym. J.* **2010**, *42*, 799; (b) Y. Lin, J. Jin, M. Song, S. J. Shaw and C. A. Stone, *Polymer* **2011**, *52*, 1716; (c) Y. Duan, S. C. Jana, A. M. Reinsel, B. Lama, M. P. Espe, *Langmuir* **2012**, *28*, 15362; (d) Y. Lin, C. A. Stone, S. J. Shaw, M. Song, *J. Appl. Polym. Sci.* **2015**, *132*, 41903; (e) A. S. Lee, S.-S. Choi, S. Y. Oh, H. S. Lee, B. Kim, S. S. Hwang, K.-Y. Baek, *J. Mater. Chem. C* **2015**, *3*, 11605.
- [13] (a) S. Yuasa, Y. Sato, H. Imoto, K. Naka, *J. Appl. Polym. Sci.* **2018**, *135*, 46033; (b) S. Yuasa, Y. Sato, H. Imoto, K. Naka, *Bull. Chem. Soc. Jpn.* **2019**, *92*, 127; (c) S. Wada, H. Imoto, K. Naka, *Bull. Chem. Soc. Jpn.* **2019**, *92*, 989.
- [14] (a) H. Imoto, Y. Nakao, N. Nishizawa, S. Fujii, Y. Nakamura, K. Naka, *Polym. J.* **2015**, *47*, 609; (b) M. Dutkiewicz, J. Karasiewicz, M. Rojewska, M. Skrzypiec, K. Dopierala, K. Prochaska, H. Maciejewski, *Chem. Eur. J.* **2016**, *22*, 13275; (c) S. Yusa, S. Ohno, T. Honda, H. Imoto, Y. Nakao, K. Naka, Y. Nakamura, S. Fujii, *RSC Adv.* **2016**, *6*, 73006; (d) H. Imoto, R. Kato, T. Honda, S. Yusa, K. Naka, *Polym. J.* **2018**, *50*, 337.
- [15] (a) M. F. Roll, J. W. Kampf, Y. Kim, E. Yi, R. M. Laine, *J. Am. Chem. Soc.* **2010**, *132*, 10171; (b) V. Ervithayasuporn, S. Chimjarn, *Inorg. Chem.* **2013**, *52*, 13108; (c) J. C. Furgal, J. H. Jung, T. Goodson III, R. M. Laine, *J. Am. Chem. Soc.* **2013**, *135*, 12259; (d) S. Chimjarn, R. Kunthom, P. Chancharone, R. Sodkhomkhum, P. Sangritrutnugul, V. Ervithayasuporn, *Dalton Trans.* **2015**, *44*, 916; (e) M. Janeta, L. John, J. Ejfler, S. Szafert, *RSC Adv.* **2015**, *5*, 72340; (f) K. Imai, Y. Kaneko, *Inorg. Chem.* **2017**, *56*, 4133; (g) P. Sangritrutnugul, T. Chaiprasert, W. Hunsiri, T. Jitjaroendee, P. Songkhum, K. Laohhasurayotin, T. Osotchan, V. Ervithayasuporn, *ACS Appl. Mater. Interfaces* **2017**, *9*, 12812.
- [16] (a) J. Guan, K. Tomobe, I. Madu, T. Goodson III, S. Jungsutiwong, R. M. Laine, *Macromolecules*, **2019**, *52*, 4008; (b) J. Guan, K. Tomobe, I. Madu, T. Goodson III, K. Makhil, T.M. Trinh, S. Rand, N. Yodsins, S. Jungsuttiwong, R. M. Laine, *Macromolecules*, **2019**, *52*, 7413.
- [17] J. Kaźmierczak, K. Kuciński, G. Hreczycho, *Inorg. Chem.* **2017**, *56*, 9337.
- [18] The results of TGA and DSC for **2a** and **2b** are shown in Figure S11.
- [19] P. S. Chung, P. H. Holloway, *J. Appl. Polym. Sci.* **2009**, *114*, 1.
- [20] S. Watase, D. Fujisaki, M. Watanabe, K. Mitamura, N. Nishioka, K. Matsukawa, *Chem. Eur. J.* **2014**, *20*, 12773.
- [21] It is reported that in the case of CC-POSS, molecular symmetry of T<sub>g</sub> affects the packing structures. For detail, see: Y. Shao, X. Xu, G.-Z. Yin, S.-Y. Han, D. Han, Q. Fu, S. Yang, W.-B. Zhang, *Macromolecules* **2019**, *52*, 2361.
- [22] Gaussian 09, Revision C.01, M. J. Frisch, G. W. Trucks, H. B. Schlegel, G. E. Scuseria, M. A. Robb, J. R. Cheeseman, G. Scalmani, V. Barone, B. Mennucci, G. A. Petersson, H. Nakatsuji, M. Caricato, X. Li, H. P. Hratchian, A. F. Izmaylov, J. Bloino, G. Zheng, J. L. Sonnenberg, M. Hada, M. Ehara, K. Toyota, R. Fukuda, J. Hasegawa, M. Ishida, T. Nakajima, Y. Honda, O. Kitao, H. Nakai, T. Vreven, J. A. Montgomery, Jr., J. E. Peralta, F. Ogliaro, M. Bearpark, J. J. Heyd, E. Brothers, K. N. Kudin, V. N. Staroverov, R. Kobayashi, J. Normand, K. Raghavachari, A. Rendell, J. C. Burant, S. S. Iyengar, J. Tomasi, M. Cossi, N. Rega, J. M. Millam, M. Klene, J. E. Knox, J. B. Cross, V. Bakken, C. Adamo, J. Jaramillo, R. Gomperts, R. E. Stratmann, O. Yazyev, A. J. Austin, R. Cammi, C. Pomelli, J. W. Ochterski, R. L. Martin, K. Morokuma, V. G. Zakrzewski, G. A. Voth, P. Salvador, J. J. Dannenberg, S. Dapprich, A. D. Daniels, Ö. Farkas, J. B. Foresman, J. V. Ortiz, J. Cioslowski, D. J. Fox, Gaussian, Inc., Wallingford CT, **2009**.
- [23] *Fluorescence Measurements, Application to bioscience, Measurement method, Series 3.* Spectroscopical Society of Japan, Academic Publication Center.

## Entry for the Table of Contents

## FULL PAPER



Two well-known open-cage silsesquioxanes, corner- and side-opened types, were compared from viewpoints of structures and materials properties. The difference in crystallinity drastically affected the OLED performance when carbazole groups were incorporated.

**Open-cage silsesquioxanes**

*H. Imoto, Y. Ueda, Y. Sato, M. Nakamura, K. Mitamura, S. Watase, K. Naka\**

**Page No. – Page No.**

**Corner- and Side-Opened Cage Silsesquioxanes: Structural Effects on the Materials Properties**